Induced pairing of fermionic impurities in a one-dimensional strongly correlated Bose gas

Michael Pasek [1,2,*] and Giuliano Orso [1,†]

[1]*Université de Paris, Laboratoire Matériaux et Phénomènes Quantiques, CNRS, F-75013 Paris, France*
[2]*Laboratoire Kastler Brossel, UPMC-Sorbonne Universités, CNRS, ENS-PSL Research University, Collège de France,
4 Place Jussieu, 75005 Paris, France*

We investigate numerically the problem of few (one or two) noninteracting spin-1/2 fermions in a shallow harmonic trap coupled via contact repulsive interactions to a uniform one-dimensional bath of lattice bosons, described by the Bose-Hubbard model. Through extensive density-matrix renormalization group calculations, we extract the binding energy and the effective mass of quasiparticles, including dressed impurities (polarons) and their two-body bound states (bipolarons), emerging from the effective nonlocal Casimir interaction between the impurities. We show that the mixture exhibits rather different pairing behaviors depending on the singlet vs triplet spin state configurations of the two fermions. For opposite spin states, bipolarons are found for any finite value of the impurity-bath coupling. In particular, in the strong-coupling regime their binding energy reduces to that of a single polaron, provided the boson-boson repulsion is not too weak. For equal spin states, we show that bipolarons emerge only beyond a critical strength of the Bose-Fermi interaction and their effective mass grows rapidly approaching the strong-coupling regime.

I. INTRODUCTION

The recent experimental realization of mixtures of Bose and Fermi superfluids in dilute cold atomic gases [1–3] has allowed us to probe the complex many-body physics of coupled interacting spin-1/2 Fermi gases and superfluid Bose gases in a variety of parameter regimes, with the possibility of controlling the lattice geometry with tailored potentials and the strength of interactions using Feshbach resonances [4]. Previous theoretical works on interacting Bose-Fermi mixtures have uncovered a variety of different ground-state phases [5–21]. One-dimensional Bose-Fermi mixtures, which show peculiar properties owing to the enhanced role of quantum fluctuations [22], have also received sustained interest [23–41].

A mobile fermionic impurity interacting with a surrounding bath of bosons is dressed by the collective excitations in the Bose gas, leading to the formation of a quasiparticle, the Bose polaron, with an enhanced effective mass [42–44]. The Bose polaron problem for a single impurity, stemming originally from the physics of electron-phonon interactions [45], has been extensively studied in recent years with ultracold atoms in one dimension [46–65] and above [66–72]. Recent experiments on impurities in a one-dimensional Bose gas [73–76] and Bose-Einstein condensates in three dimensions [77–80] have also been performed, with successful measurements of the polaron self-energy, which can be extracted from spectroscopy measurements [78], and the effective polaronic

mass, by monitoring dipole oscillations of the impurity in a harmonic trap [74].

The natural extension of these works on the Bose polaron problem for a single impurity is the study of a few interacting impurities coupled to a common bath. This longstanding problem, first addressed in ^{3}He-^{4}He mixtures [81], was recently studied theoretically in one-dimensional [82–86] and three-dimensional [87–89] cold atomic gases. Static and mobile impurities in one-dimensional quantum fluids are of particular interest because of the emergence of an effective attractive Casimir interaction between impurities due to the exchange of phononic excitations in the bath [90–95]. Hence, two impurities can form a new bosonic bound state, the bipolaron, a quasiparticle state that has been studied in the context of high-T_c superconductivity [96–98].

In this work, we investigate the polaron problem for one and two fermionic impurities interacting with a one-dimensional Bose gas in a tight optical lattice described by the Bose-Hubbard model. Based on the density-matrix renormalization group (DMRG) [99,100] method, we compute the ground-state energy of the mixture in the presence of a shallow harmonic potential for the impurities as a function of the trapping frequency. This allows us to extract the binding energy and effective mass of both polarons and bipolarons with great accuracy. For bipolarons, we show that these quantities exhibit distinct properties depending on the spin configuration, singlet or triplet, of the two constituent fermions. Our numerical approach goes beyond mean-field and variational calculations and provides a competing alternative to quantum Monte Carlo methods [63,64] to probe the Bose polaron problem in one-dimensional systems.

Although purely induced pairing of trapped bosonic impurities coupled to a one-dimensional bath was recently addressed theoretically [82], the underlying pairing mechanism

---

*Present address: Institut für Theoretische Physik, Goethe-Universität, 60438 Frankfurt am Main, Germany; pasek@th.physik.uni-frankfurt.de

†giuliano.orso@univ-paris-diderot.fr

was essentially due to mean-field effects of the impurities on a trapped ideal Bose gas and not due to the exchange of phononic modes, which were absent. Moreover, no pairing between fermionic impurities was observed in this work.

This paper is organized as follows. In Sec. II we present the microscopic model Hamiltonian used to describe the Bose-Fermi mixture. In Sec. III we start by introducing our theoretical approach to compute the binding energy and effective mass of a single polaron. We then present our numerical results based on the DMRG method and compare them with analytical predictions from Bogoliubov theory in the regime of weak Bose-Fermi coupling. In Sec. IV we extend this approach to bipolarons and present numerical results for the binding energy and effective mass, distinguishing the cases of two impurities with equal and opposite spins.

II. MODEL HAMILTONIAN

We describe the one-dimensional Bose-Fermi mixture by a lattice Hamiltonian consisting of three parts, $\hat{H} = \hat{H}_b + \hat{H}_f + \hat{H}_{bf}$. The first term corresponds to the Bose-Hubbard model

$$\hat{H}_b = -t_b \sum_{\langle i,j \rangle} \hat{b}_i^\dagger \hat{b}_j + \frac{U_b}{2} \sum_i \hat{n}_{ib}(\hat{n}_{ib} - 1), \quad (1)$$

describing bosons hopping between neighboring sites with tunneling rate t_b and subject to on-site repulsive interactions of strength $U_b > 0$.

Importantly, we assume in this work that the spin-1/2 fermions have no *direct* intraspecies interaction, while effective interactions between fermions will be generated dynamically via the exchange of bosonic density fluctuations. We also consider that fermions are trapped at the center of the chain by a harmonic potential. In the absence of coupling to the bosons, they obey the Hamiltonian

$$\hat{H}_f = -t_f \sum_{\langle i,j \rangle, \sigma} \hat{c}_{i\sigma}^\dagger \hat{c}_{j\sigma} + \sum_{i,\sigma} \frac{1}{2} m^* \omega^2 \left(i - \frac{L}{2} \right)^2 \hat{n}_{i\sigma}, \quad (2)$$

where $\sigma = \uparrow, \downarrow$ accounts for the two spin states, t_f is the fermion hopping rate, $m^* = 1/(2t_f)$ is the bare fermionic mass in the lattice, ω is the trapping frequency, and L is the size of the chain. Here both $\hbar$ and the lattice period have been set to unity.

Finally, boson and fermion densities are coupled by the following Hubbard-like term:

$$\hat{H}_{bf} = U_{bf} \sum_{i,\sigma} \hat{n}_{ib} \hat{n}_{i\sigma}, \quad (3)$$

where U_{bf} is the strength of the Bose-Fermi interaction, which we assume is always repulsive, $U_{bf} > 0$.

In this work, we assume that the boson density $n_b = N_b/L$ is finite, with $N_b = \sum_i \langle \hat{n}_{ib} \rangle$ being the total number of bosons in the system. The strength of boson-boson interactions in the Bose gas can then be characterized via the dimensionless Lieb-Liniger parameter $\gamma = U_b/(2n_b t_b)$ [22,53]. In contrast, the total number of fermions per spin component, $N_\sigma = \sum_i \langle \hat{n}_{i\sigma} \rangle$, is chosen to be finite and small, corresponding to the picture of a few (one or two) fermionic impurities moving in a bath of correlated bosons. For simplicity, in the following we restrict our discussion to equal hopping amplitudes of the

fermionic and bosonic components and fix the energy scale by setting $t_f = t_b = 1$.

The impurity trapping potential in Eq. (2) allows us to extract the binding energy and effective mass of polarons and bipolarons in a uniform system by carrying out DMRG calculations of the ground-state energy of the mixture for different values of the trap frequency and performing a scaling analysis, as discussed in Secs. III and IV. The use of DMRG to extract the polaron mass through a finite-size scaling analysis was first investigated for the one-dimensional Holstein model [101]. Since our DMRG method requires open boundary conditions, we find that, in the absence of the trapping potential ($\omega = 0$), the mobile impurity in its ground state binds at the edge of the chain, where the density of the bath is lower than its bulk value [57,82,102]. To avoid such strong finite-size effects, we restrict our calculations to finite ω values that keep the impurities in the middle of the chain.

III. SINGLE IMPURITY

We first consider the properties of a single polaron, obtained by immersing a single fermionic impurity in the bosonic bath. For definiteness, we choose the impurity to have spin up, i.e., $N_\uparrow = 1, N_\downarrow = 0$.

A. Trap scaling approach for polarons

Let us assume, for the time being, that there is no trapping potential, $\omega = 0$, and that the length of the chain is infinite, so that the lattice Hamiltonian of the coupled system is translationally invariant.

Let $E_q^\uparrow$ be the lowest energy of the mixture for a given momentum q of the polaron. For small q, this energy can be Taylor expanded as

$$E_q^\uparrow \simeq E_0^\uparrow + \frac{q^2}{2m_p^*} + A^\uparrow q^4, \quad (4)$$

where $E_0^\uparrow$ represents the absolute ground-state energy, m_p^* represents the polaron effective mass, and $A^\uparrow$ is a numerical constant accounting for anharmonic terms in the polaron energy dispersion. The binding energy μ_p of the polaron is defined as

$$\mu_p = E_0^\uparrow - \left(E_{\text{gs}}^b - 2 \right), \quad (5)$$

where E_{gs}^b is the ground-state energy of the interacting Bose gas in the absence of impurities and the last term corresponds to the ground-state energy of a free fermionic impurity with the energy dispersion relation $\epsilon_q^f = -2\cos q$. In the absence of Bose-Fermi coupling, we have $E_q^\uparrow = E_{\text{gs}}^b + \epsilon_q^f$, implying that the binding energy of the polaron vanishes, i.e., $\mu_p = 0$. Since $\epsilon_q^f \simeq -2 + q^2 - q^4/12$, the polaron effective mass reduces to the bare mass of the impurity, $m_p^* = 1/2 = m^*$, as expected, and $A^\uparrow = -1/12$.

Let us now consider a finite trap frequency ω for the impurity, and let $E_{\text{gs}}^\uparrow$ be the corresponding ground-state energy of the mixture that we compute using the DMRG method. For small values of ω, it follows from Eqs. (2) and (4) that $E_{\text{gs}}^\uparrow$ is well approximated by the ground-state energy of the following anharmonic quantum oscillator Hamiltonian in the

first-quantized form:

$$H_{\mathrm{an}}^{\uparrow} = E_0^{\uparrow} + \frac{q^2}{2m_p^*} + \frac{1}{2}m^*\omega^2 x^2 + A^{\uparrow}q^4, \qquad (6)$$

where $x = i - L/2$ represents the continuum spatial coordinate of the impurity. By treating the anharmonic term in Eq. (6) within first-order perturbation theory, we obtain

$$E_{\mathrm{gs}}^{\uparrow} \simeq E_0^{\uparrow} + \tfrac{1}{2}\omega_p + \tfrac{3}{4}m_p^{*2}A^{\uparrow}\omega_p^2, \qquad (7)$$

where $\omega_p = \omega\sqrt{m^*/m_p^*}$ is the effective trap frequency for the polaron. This corresponds to the frequency of the dipole oscillation that can be generated experimentally by displacing the trap center of the fermionic impurity, provided that the boson density is kept uniform [103].

Equation (7) suggests that the binding energy and the effective mass of the polaron can be inferred by calculating the ground-state energy $E_{\mathrm{gs}}^{\uparrow}$ of the coupled system for several (small) values of the trap frequency ω and fitting the obtained results via a quadratic polynomial,

$$p(\omega) = a_0 + a_1\omega + a_2\omega^2, \qquad (8)$$

where a_0, a_1, and a_2 are fitting coefficients. By comparing Eq. (8) with Eq. (7), we find $E_0^{\uparrow} = a_0$ and $m^*/m_p^* = 4a_1^2$. After this trap scaling procedure, the polaron binding energy μ_p is evaluated from Eq. (5) using the fitted value of $E_0^{\uparrow}$ as well as the ground-state energy of the bosonic bath E_{gs}^b (which is independent of ω). The specific range of ω values to be used for the fit depends on the system size L and the boson-fermion coupling strength U_{bf}. To avoid finite-size effects, the density distribution of the fermionic impurity must decay sufficiently fast near the edge of the chain, which yields a lower bound on the trap frequency for a given value of L and U_{bf}.

B. Results

In Fig. 1, we show examples of the density profiles of the bosonic bath [Fig. 1(a)] and of the fermionic impurity [Fig. 1(b)] calculated for different values of the trap frequency ω. Here $L = 80$, $n_b = 2$, $U_b = 2$, and $U_{bf} = 6$. We see that the boson local density is strongly depleted in the center of the chain, where the fermionic impurity is trapped. In Fig. 1(c), we display the calculated values of the ground-state energy of the coupled system as a function of the trap frequency, together with the fitted polynomial (8). We see that the latter reproduces quite accurately the numerical data in the low-frequency regime. The fitting coefficient a_2 is typically small (this will no longer be true for bipolarons; see Sec. IV). Taking into account that the calculated ground-state energy of the Bose gas alone is $E_{\mathrm{gs}}^b = -70.1557$, we find that the polaron binding energy for the above parameters is $\mu_p = 6.853$, while the obtained value for the inverse effective mass ratio is $m^*/m_p^* = 0.242$.

We repeat the above procedure for different values of the boson-fermion coupling U_{bf} and for two values of the intra-bath interaction strength, $U_b = 2$ and $U_b = 4$. The obtained results for the polaron binding energy are plotted in Fig. 2 as a function of U_{bf}. We see from Fig. 2 that the polaron binding energy gets bigger as the coupling to the bath increases,
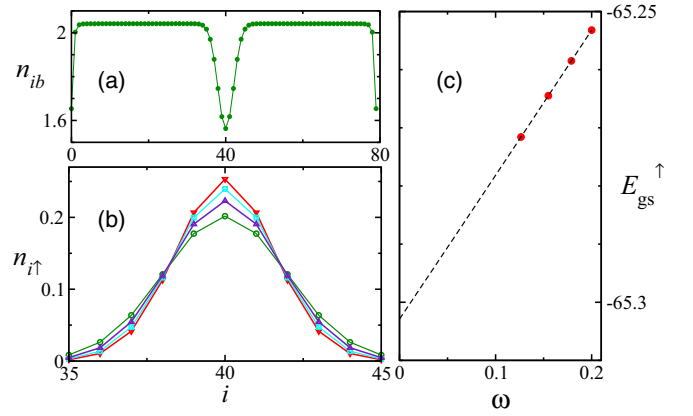

FIG. 1. A single fermionic impurity immersed in a one-dimensional Bose gas and trapped at the center of the chain by a shallow harmonic potential of frequency ω. (a) Local density distribution of bosons n_{ib} for $\omega = 0.1265$. (b) Fermionic density profile $n_{i\uparrow}$ near the trap center plotted for different values of the trap frequency, $\omega = 0.1265$ (circles), 0.1549 (upward triangles), 0.1789 (squares), and 0.2 (downward triangles). (c) Ground-state energy $E_{\mathrm{gs}}^{\uparrow}$ of the coupled system as a function of the trap frequency. The dashed line is the quadratic polynomial, $p(\omega) = a_0 + a_1\omega + a_2\omega^2$, with fitted parameters $a_0 = -65.3029$, $a_1 = 0.246$, and $a_2 = 0.0123$. The length of the chain is $L = 80$, and the boson density is $n_b = 2$. Tunneling rates of bosons and fermions are set to $t_b = t_f = 1$. Boson-boson and boson-fermion interaction strengths are $U_b = 2$ and $U_{bf} = 6$, respectively.

in agreement with previous quantum Monte Carlo studies [63,64].

For weakly interacting bosons, the numerical results can be compared against analytical calculations based on Bogoliubov theory by treating the Bose-Fermi interaction U_{bf} as a small perturbation, as previously done for the continuum [63,68].
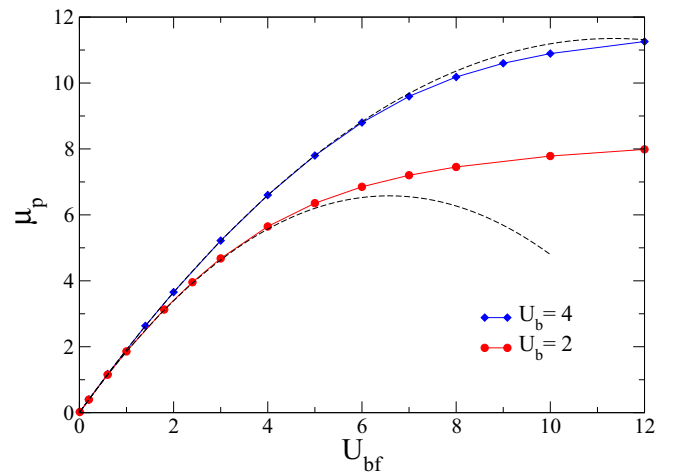

FIG. 2. Binding energy μ_p of the polaron, Eq. (5), as a function of the impurity-bath interaction strength U_{bf}, plotted for two different values of the boson-boson repulsion, $U_b = 2$ ($\gamma = 0.5$, red circles) and $U_b = 4$ ($\gamma = 1$, blue diamonds). The boson density is set to $n_b = 2$. Dashed lines correspond to the predictions from Bogoliubov theory [see Eq. (10)].
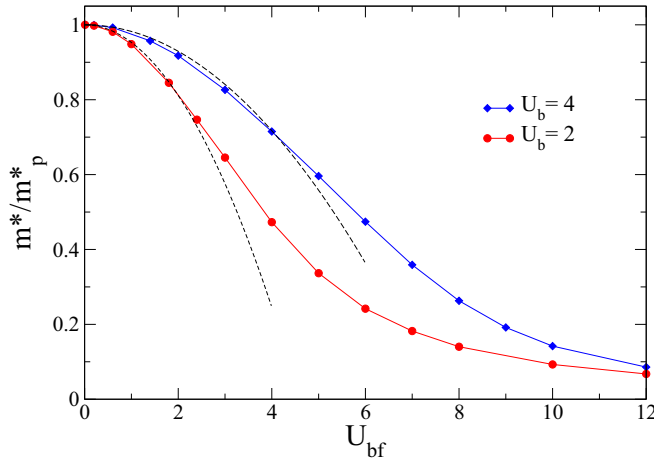
FIG. 3. Inverse effective mass ratio m^*/m_p^* of the polaron as a function of the impurity-bath interaction strength U_{bf}, plotted for two different values of the boson-boson repulsion, $U_b = 2$ ($\gamma = 0.5$, red circles) and $U_b = 4$ ($\gamma = 1$, blue diamonds). The boson density is set to $n_b = 2$. Dashed lines correspond to the prediction from Bogoliubov theory [see Eq. (13)].

Up to second-order terms, one finds

$$\mu_p^{\text{bog}} = U_{bf}n_b - (U_{bf}\sqrt{n_b})^2 \frac{1}{L} \sum_k (u_k + v_k)^2 \frac{1}{\epsilon_{-k}^f - \epsilon_0^f + \omega_k}, \tag{9}$$

where the first term on the right-hand side corresponds to the mean-field result, while the second term is the correction coming from density fluctuations in the bath. The Bogoliubov coefficients u_k, v_k satisfy $u_k^2 = 1 + v_k^2 = (\bar{\epsilon}_k + U_b n_b + \omega_k)/(2\omega_k)$ and $u_k v_k = -U_b n_b/(2\omega_k)$, where $\epsilon_k^b = \epsilon_k^f$ and $\omega_k = (\bar{\epsilon}_k^2 + \bar{\epsilon}_k 2n_b U_b)^{1/2}$ is the energy of the elementary excitations, with $\bar{\epsilon}_k = 2(1 - \cos k)$. By taking into account that $(u_k + v_k)^2 = \bar{\epsilon}_k/\omega_k$ and replacing the sum over quasimomenta in Eq. (9) by an integral, we obtain

$$\mu_p^{\text{bog}} = U_{bf}n_b - \frac{U_{bf}^2}{U_b}\left(\frac{1}{2} - \frac{1}{\pi}\arctan\sqrt{\frac{2}{n_b U_b}}\right). \tag{10}$$

In the continuum limit, $n_b U_b \to 0$, Eq. (10) reduces to $\mu_p^{\text{bog}} \simeq n_b U_{bf} - \frac{U_{bf}^2}{\pi}\frac{1}{\sqrt{\gamma}}m^*$, where m^* is the bare mass of the impurity [63].

We see from Fig. 2 that the Bogoliubov prediction reproduces properly our numerical results for the binding energy in the regime of weak Bose-Fermi coupling but significantly deviates from them in the strong-coupling regime, in particular when the boson-boson interaction strength is small. This is not surprising, as in this limit the second term on the right-hand side of Eq. (10) becomes dominant over the mean-field correction, and perturbation theory ceases to be valid.

An important effect of the coupling to the bosonic bath is the enhancement of the effective mass m_p^* of the fermionic impurity compared to its bare mass m^*, as shown in Fig. 3. The corresponding Bogoliubov prediction for the inverse of

the polaron effective mass can be written as

$$\frac{1}{m_p^{*\text{bog}}} = \frac{1}{m^*} + \frac{\partial^2 \mu_p^{\text{bog}}(q)}{\partial q^2}\bigg|_{q=0}, \tag{11}$$

where

$$\mu_p^{\text{bog}}(q) = U_{bf}n_b - U_{bf}^2 n_b \int_{-\pi}^{\pi} \frac{dk}{2\pi}(u_k + v_k)^2 \frac{1}{\epsilon_{q-k}^f - \epsilon_q^f + \omega_k} \tag{12}$$

is the generalization of the Bogoliubov prediction for the binding energy of the impurity, Eq. (10), under the new assumption that the impurity carries a finite quasimomentum q.

We then differentiate twice the right-hand side of Eq. (12) with respect to q and calculate analytically the integral over momentum for $q = 0$. From Eq. (11) we obtain

$$\frac{1}{m_p^{*\text{bog}}} = 2 - U_{bf}^2\frac{n_b}{2\pi}\frac{4\pi + 2\sqrt{2x}(x - 2) - 8\arctan\sqrt{\frac{2}{x}}}{x^3}, \tag{13}$$

with $x = n_b U_b$. In the continuum limit, $n_b U_b \to 0$, Eq. (13) reduces to $m^*/m_p^{*\text{bog}} = 1 - 2\eta^2/(3\pi\gamma^{3/2})$, with $\eta = U_{bf}/(2n_b t_b)$, in agreement with previous work [63]. Since there is no mean-field correction for the polaron effective mass, the Bogoliubov prediction works better for weak boson-boson interactions, as shown in Fig. 3 by the dashed lines.

IV. TWO IMPURITIES

We now investigate the formation of bound states of two fermionic impurities, i.e., bipolarons, which are induced solely by the exchange of density fluctuations in the bosonic bath [5–9]. In this aim, we first generalize the trap scaling procedure introduced in Sec. III to bipolarons. We then use this approach to compute the binding energy and effective mass of bipolarons for both the singlet ↑↓ spin configuration (corresponding to $N_\uparrow = N_\downarrow = 1$) and the triplet ↑↑ spin configuration ($N_\uparrow = 2, N_\downarrow = 0$).

A. Trap scaling approach for bipolarons

We proceed as in Sec. III by first assuming that there is no trapping potential [i.e., we set $\omega = 0$ in Eq. (2)] and that the length of the chain is infinite. Let E_Q be the lowest energy level of the mixture containing a bipolaron with center-of-mass quasimomentum Q. In analogy to Eq. (4), for small Q we can write

$$E_Q \simeq E_0 + \frac{Q^2}{2M_{\text{bip}}^*} + AQ^4, \tag{14}$$

where E_0 is the ground-state energy of the uniform mixture, M_{bip}^* is the bipolaron effective mass, and A is a numerical coefficient accounting for anharmonic terms in the dispersion relation. The binding energy E_b of the bipolaron is then defined as

$$-E_b = E_0 - 2E_0^\uparrow + E_{\text{gs}}^b, \tag{15}$$

where the minus sign on the left-hand side of Eq. (15) ensures that $E_b \geqslant 0$.

We now discuss the effect of a shallow harmonic trap acting on the two fermionic impurities. Let E_{gs} be the corresponding ground-state energy of the mixture, and let $x_1 = i - L/2$, $x_2 = j - L/2$ be the spatial coordinates of the two fermions measured with respect to the center of the chain. In the first-quantization formalism, the total external potential acting on the impurities can be written as

$$\frac{1}{2}m^*\omega^2\left(x_1^2 + x_2^2\right) = \frac{1}{2}2m^*\omega^2 R^2 + \frac{1}{2}\frac{m^*}{2}\omega^2 r^2, \quad (16)$$

where $R = (x_1 + x_2)/2$ and $r = x_1 - x_2$ represent the center-of-mass and the relative motion coordinates, respectively. For bound states, the mean distance between the two constituent particles is finite, $\sqrt{\langle r^2 \rangle} < +\infty$, implying that the effect of a shallow trap on the relative motion is perturbative. Hence, for a small enough trap frequency, E_{gs} is given by the ground-state energy of the following Hamiltonian:

$$H_{\mathrm{an}} = E_0 + \frac{1}{4}m^*\omega^2\langle r^2 \rangle + \frac{Q^2}{2M_{\mathrm{bip}}^*} + \frac{1}{2}2m^*\omega^2 R^2 + AQ^4, \quad (17)$$

where the last term can again be evaluated within first-order perturbation theory. This yields

$$E_{\mathrm{gs}} \simeq E_0 + \tfrac{1}{2}\omega_{\mathrm{bip}} + \left(\tfrac{3}{4}M_{\mathrm{bip}}^{*\,2}A + \tfrac{1}{8}M_{\mathrm{bip}}^*\langle r^2 \rangle\right)\omega_{\mathrm{bip}}^2, \quad (18)$$

where $\omega_{\mathrm{bip}} = \omega\sqrt{2m^*/M_{\mathrm{bip}}^*}$ is the effective trap frequency for the bipolaron. As previously done for the single-polaron problem, we compute the ground-state energy of the mixture for different (small) values of the trap frequency ω and fit the obtained results via a quadratic polynomial,

$$\tilde{p}(\omega) = \alpha_0 + \alpha_1\omega + \alpha_2\omega^2, \quad (19)$$

where α_i are fitting parameters. From this, we obtain the ground-state energy $E_0 = \alpha_0$ of the uniform mixture, as well as the inverse effective mass ratio $2m^*/M_{\mathrm{bip}}^* = 4\alpha_1^2$ of the bipolaron. The binding energy E_b is then evaluated from Eq. (15).

We emphasize that Eq. (18) relies on the assumption that the effect of the trap on the relative motion of the two impurities is *perturbative* and therefore contributes only to the ω^2 term in E_{gs}. As a consequence, our fitting procedure is accurate only if the binding energy of the bipolaron is large compared to the trap frequency, i.e., $E_b \gg \omega$. At the breaking point of the molecule, the average size of the molecule diverges, and the right-hand side of Eq. (18) becomes ill defined. In order to satisfy the condition $E_b \gg \omega$, we would need to consider smaller and smaller values of the trap frequency. To avoid the pinning of the impurities at the edge of the system, this in turn requires simulations of larger and larger systems. Numerically accurate results in this regime are therefore challenging.

We have benchmarked the trap scaling procedure for two simpler one-dimensional systems: two fermions with opposite spins obeying the attractive Fermi-Hubbard model and two identical fermions described by the attractive t-V model. In both cases we have recovered the known analytical results [104] for the bound state *in the absence of the trap*.

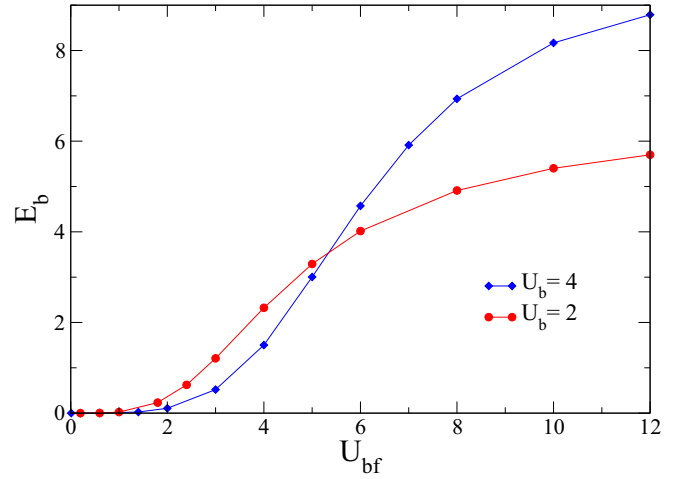

FIG. 4. Binding energy E_b of the $\uparrow\downarrow$ bipolaron [see Eq. (15)] as a function of the impurity-bath interaction strength U_{bf}. The two data sets correspond to two different values of the boson-boson interaction, $U_b = 2$ (red circles) and $U_b = 4$ (blue diamonds). The boson density is set to $n_b = 2$.

B. Results: $\uparrow\downarrow$ bipolaron

In Fig. 4, we show the numerical results for the binding energy of the $\uparrow\downarrow$ bipolaron as a function of the impurity-bath interaction U_{bf} for two different values of the intrabath interaction, $U_b = 2$ and 4, with the boson density fixed to $n_b = 2$. The bipolaron binding energy is found to be always positive for any finite value of the impurity-bath coupling. This is consistent with the fact that in one dimension any attractive contact interaction produces a two-body bound state, leading to a BCS instability [105].

As shown in Fig. 4, the binding energy E_b increases monotonously with the impurity-bath coupling U_{bf} and tends to saturate for $U_{bf} \to +\infty$. In the regime of weak impurity-bath coupling, we also find that the binding energy of the bipolaron decreases as the boson-boson interaction U_b gets larger. This is due to the fact that bosonic density fluctuations, which mediate the effective attractive interaction between the two impurities, are progressively reduced as the level of correlation in the bath rises. Indeed, in the limit of large U_b, i.e., deep in the Mott regime for integer fillings [22], the bosonic bath acts as a uniform external potential for the fermions, and hence, the pair binding energy vanishes in the absence of a direct interaction between the two impurities (in the fermionized limit $U_b \to +\infty$, it was previously pointed out that two spin-polarized fermionic impurities interacting with the fermionized gas cannot form a bound state in the continuum, although two bosonic impurities can [40,106]).

In the opposite limit of strong coupling with the bath, the tendency is reversed; namely, the binding energy becomes larger for stronger boson-boson interaction, as can be seen in Fig. 4. This can be attributed to the fact that for $U_{bf} \gg U_b \gg 1$, the $\downarrow$ fermion can occupy the same hole as previously created in the bosonic bath to host the $\uparrow$ fermion without any significant additional energy cost, so that $E_0 \simeq E_0^\uparrow$. From Eqs. (15) and (5), this implies that
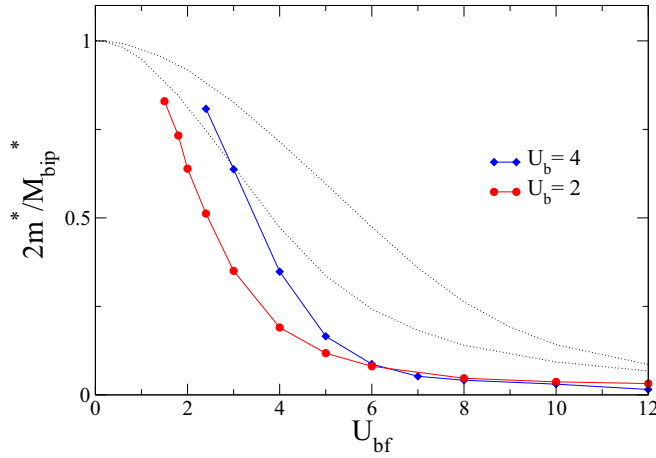
$$E_b \simeq \mu_p - 2 \quad (20)$$

FIG. 5. Inverse effective mass ratio of the ↑↓ bipolaron as a function of the impurity-bath interaction strength. The two data sets correspond to two different values of the boson-boson interaction, $U_b = 2$ (red circles) and $U_b = 4$ (blue diamonds). The boson density is set to $n_b = 2$. The dotted lines represent the corresponding effective mass ratios for the single polaron, which are reproduced from Fig. 3. For small values of U_{bf}, we do not display any numerical data points as our fitting procedure to extract $M_{\rm bip}^*$ becomes inaccurate due to finite-size effects (see text). In this regime the mass ratios of the polaron and bipolaron approach each other.

and thus that E_b should increase with growing U_b (see Fig. 2), in full agreement with our numerics.

In Fig. 5, we display the corresponding results for the inverse effective mass ratio of the ↑↓ bipolaron for the same set of system parameters. On general grounds, it is expected that the effective mass of the molecule increases as its binding energy builds up (see Fig. 4). This is indeed what we find, as for weak Bose-Fermi coupling the effective mass $M_{\rm bip}^*$ is reduced for increasing boson-boson repulsion, while in the opposite regime of strong coupling, $U_{bf} \gg 1$, the tendency is reversed. In particular, we see by comparison between Figs. 4 and 5 that the two curves cross at similar values of the impurity-bath coupling (around $U_{bf} = 6$).

In Fig. 5, we do not display results for small values of U_{bf}, where the binding energy of the bipolaron (see Fig. 4) becomes comparable to or smaller than the trap frequency, $|E_b| \lesssim \omega$. In this regime the effect of the harmonic trap is not perturbative, and our fitting procedure to extract $M_{\rm bip}^*$ is no longer accurate. As this occurs, the bipolaron effective mass $M_{\rm bip}^*$ is already close to the sum of the mass of its constituents $2m_p^*$, i.e., twice the effective mass of a single polaron, as indicated in Fig. 5 by the dotted lines.

In the left panel of Fig. 6, we show the dependence of the fitting coefficient α_2 on the coupling strength U_{bf} for the case $U_b = 2$ ($U_b = 4$ yields similar results). Due to the finite harmonic oscillator length of the trap, we see that α_2 does not diverge as U_{bf} approaches zero as expected from the divergence of the bound state size $\langle r^2 \rangle$ but reaches a maximum and then decreases until it turns negative. This stems from the fact that at $U_{bf} = 0$, where no bound state exists, one is left with the problem of two noninteracting lattice fermions in a harmonic potential. In a previous work [107], an analytical formula was found for the perturbative
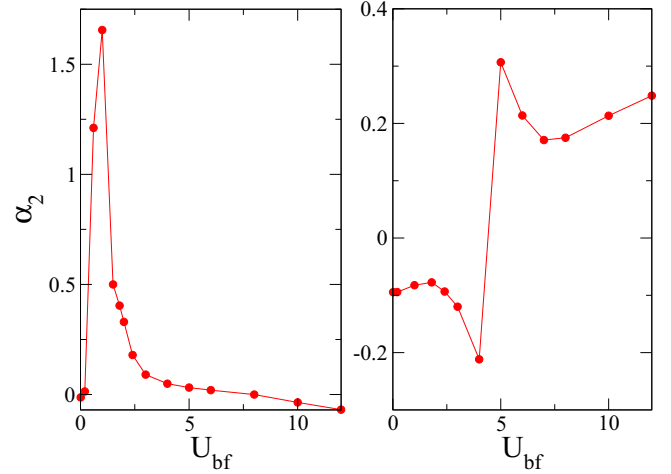

FIG. 6. Fitting coefficient α_2 [see Eq. (19)] as a function of the Bose-Fermi interaction strength U_{bf} for the ↑↓ bipolaron (left panel) and for the ↑↑ bipolaron (right panel). The system size is $L = 80$. The boson-boson repulsion is set to $U_b = 2$, while the boson density is $n_b = 2$.

expansion of the single-particle energy levels of the quantum harmonic oscillator on a lattice as a function of the trap frequency ω. For two fermions with opposite spins we find that $\alpha_1 = 1$ and $\alpha_2 = -1/32$, whereas for equal spins $\alpha_1 = 2$ and $\alpha_2 = -3/32$ (in both cases $\alpha_0 = -4$). These limiting results are in full agreement with our numerical results displayed in Fig. 6.

C. Results: ↑↑ bipolaron

Let us now consider the case of two fermionic impurities with the same spin state. Despite the Pauli exclusion principle which forbids any contact interaction between the two impurities, the formation of bipolarons is nevertheless possible owing to the nonlocal nature of the phonon-mediated interactions [90–95], although the typical values of their pair binding energy are smaller than in the spin singlet configuration.

Importantly, we find that for the ↑↑ bipolaron formation a finite-size scaling analysis is crucial to obtain meaningful results. As an example, in Fig. 7 we plot the values of the pair binding energy, calculated via the trap scaling procedure, as a function of the inverse size of the chain $1/L$ for two different values of the Bose-Fermi coupling. All the obtained values of the pair binding energy shown in Fig. 7 are negative, indicating the presence of strong finite-size effects. However, both data sets show a linear dependence on $1/L$, and the intercept of the curves with the y axis yields the extrapolated value of the pair binding energy in the thermodynamic limit, $L \to +\infty$. For $U_{bf} = 4$, the y intercept is vanishingly small, signaling the absence of bipolarons, whereas for $U_{bf} = 5$ the y intercept is finite and positive, implying that a bipolaron has formed in the system. Hence, we find that impurities with equal spins form a spin-triplet bound state only above a finite critical interaction strength U_{bf}^c, in sharp contrast to the singlet case. As shown in the right panel of Fig. 6, the value of the coefficient α_2 changes from negative to positive in the vicinity
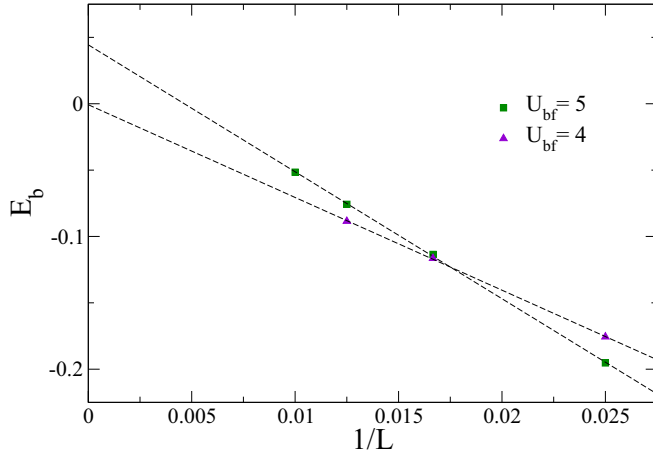
FIG. 7. Binding energy of the $\uparrow\uparrow$ bipolaron as a function of the inverse system size $1/L$ for two different values of the Bose-Fermi coupling, $U_{bf} = 4$ (triangles) and $U_{bf} = 5$ (squares). The bosonic bath parameters are $n_b = 2$ and $U_b = 2$, and the length of the chain varies from $L = 40$ to $L = 100$. The numerical data are well fitted with a straight line, whose y intercept yields an estimate of E_b in the infinite system. For $U_{bf} = 4$ the y intercept vanishes, signaling the absence of a bound state at low U_{bf}.

of the critical point, providing a simple way to approximately estimate its position.

In Fig. 8, we display the pair binding energy for the $\uparrow\uparrow$ triplet bipolaron state as a function of the Bose-Fermi coupling strength using the same set of parameters as for the single-polaron case. We see that mixtures with strongly correlated bosons require a larger value of the critical Bose-Fermi interaction U_{bf}^c for the formation of triplet polaron pairs to happen, in agreement with early bosonization studies [25]. A recent theoretical study on fermionic impurities in three-dimensional Bose-Einstein condensates found a similar
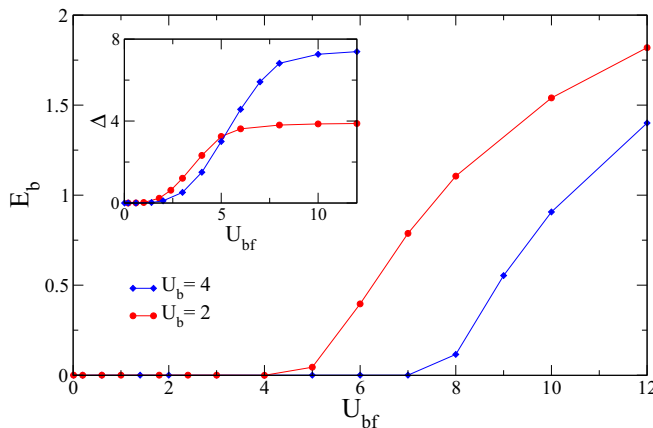

FIG. 8. Pair binding energy E_b of the $\uparrow\uparrow$ bipolaron, extrapolated to infinite system size (see Fig. 7), as a function of the impurity-bath interaction for two values of the boson-boson repulsion, $U_b = 2$ (red circles) and $U_b = 4$ (blue diamonds). The boson density is $n_b = 2$. The bipolaron is formed only beyond a finite critical value of the impurity-bath coupling U_{bf}^c. Inset: Spin energy gap Δ of bipolarons [see Eq. (21)] versus Bose-Fermi coupling.
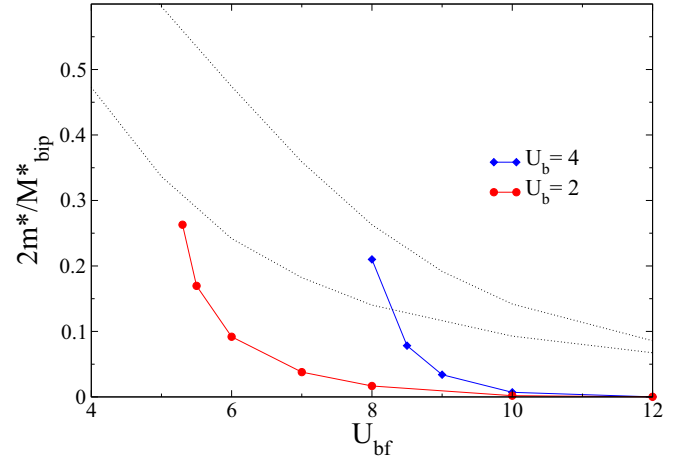

FIG. 9. Inverse effective mass ratio of the $\uparrow\uparrow$ bipolaron as a function of the impurity-bath interaction strength U_{bf}. The two data sets correspond to two different values of the boson-boson interaction, $U_b = 2$ (red circles) and $U_b = 4$ (blue diamonds). The boson density is set to $n_b = 2$. The dotted lines represent the corresponding effective mass ratios for the single polaron, reproduced from Fig. 3. Close to the breaking point of the bipolaron state (see Fig. 8), where the mass ratios of the polaron and bipolaron approach each other, our numerical data are biased by finite-size effects and are therefore not shown (see text).

dependence of the p-wave critical interaction strength on the bath interaction parameter [89]. We see from Fig. 8 that, for a fixed value of U_{bf}, the pair binding energy is inversely proportional to the intrabath interaction strength U_b. Unlike that for the $\uparrow\downarrow$ singlet bipolaron, this behavior extends in the strong-coupling regime of large U_{bf}, where the pair binding energy saturates to $E_b \simeq 2.34$ and $E_b \simeq 1.89$ for $U_b = 2$ and $U_b = 4$, respectively (not shown in Fig. 8). Since the Pauli exclusion principle prevents the two fermionic impurities with equal spin from sharing the same site, two different holes in the bosonic bath have to be created at neighboring sites to accommodate the impurities. As a consequence, the simple relation between the binding energies of the polaron and the bipolaron in Eq. (20) does not hold for the $\uparrow\uparrow$ bipolaron.

It is also interesting to investigate the spin gap associated with the bipolaron state, which is defined as the difference between the pair binding energies of the singlet and triplet spin configurations:

$$\Delta = E_b^{\uparrow\downarrow} - E_b^{\uparrow\uparrow}. \tag{21}$$

Our numerical results for the spin gap are displayed in the inset of Fig. 8. We see that Δ becomes nearly constant once the $\uparrow\uparrow$ bipolaron formation sets in for $U_{bf} > U_{bf}^c$.

In Fig. 9, we show the corresponding results for the effective mass ratio $2m^*/M_{\text{bip}}^*$ of the $\uparrow\uparrow$ bipolaron as a function of the Bose-Fermi coupling. Near the breaking point of the bound state, $U_{bf} = U_{bf}^c$, we find that the effective mass ratio of the bipolaron approaches that of the single polaron, m^*/m_p^*. By comparing Fig. 9 with Fig. 5, we see that the effective mass of the bipolaron in the triplet state increases much faster with the Bose-Fermi coupling than the effective mass of the singlet state. This interesting effect can be understood

from the fact that the motion of the ↑↑ bipolaron requires a significant rearrangement of the bosonic bath in order to shift the two neighboring holes hosting the bound state, resulting in increased inertia.

V. CONCLUSIONS

To summarize, we have presented a thorough numerical study of a few noninteracting spin-1/2 fermions coupled to a one-dimensional gas of correlated lattice bosons. We found that despite the absence of direct attractive interaction between the impurities, the latter can bind in pairs through the exchange of density fluctuations in the bosonic bath. In order to fully characterize the ground-state properties of this system, the binding energy and the effective mass of both polarons and bipolarons have been investigated numerically through accurate DMRG calculations based on a trap scaling procedure.

For the bipolaron state, we have shown that the binding energy and effective mass exhibit qualitatively different behaviors depending on the spin state of the two impurities. For opposite spin states, a bipolaron bound state exists for any finite value of the impurity-bath (or Bose-Fermi) coupling, while for impurities with equal spin states, bipolarons appear only beyond a critical value of the coupling strength to the bath. In the ↑↓ (singlet) spin configuration, the dependence of the binding energy and effective mass of the bipolaron on the bath interaction parameter exhibits opposite trends in the weak- and strong-coupling regimes, a feature not present in the ↑↑ triplet spin configuration. Furthermore, we found that for equal spin states the effective mass of the bipolaron, once formed, grows much faster as the strong-coupling regime is approached than in the singlet spin configuration.

Our results can be tested in future experiments on bipolarons in one-dimensional Bose-Fermi mixtures of ultracold atoms. We believe that the whole parameter space that we studied here should be accessible to experiments, as the impurity-bath Bose-Fermi coupling can be tuned via a Feshbach resonance, while the interaction parameter of the bosonic bath can be controlled by changing the depth of the optical lattice in the longitudinal direction.

[1] I. Ferrier-Barbut, M. Delehaye, S. Laurent, A. T. Grier, M. Pierce, B. S. Rem, F. Chevy, and C. Salomon, A mixture of Bose and Fermi superfluids, Science **345**, 1035 (2014).

[2] M. Delehaye, S. Laurent, I. Ferrier-Barbut, S. Jin, F. Chevy, and C. Salomon, Critical Velocity and Dissipation of an Ultracold Bose-Fermi Counterflow, Phys. Rev. Lett. **115**, 265303 (2015).

[3] R Onofrio, Cooling and thermometry of atomic Fermi gases, Phys. Usp. **59**, 1129 (2016).

[4] I. Bloch, J. Dalibard, and W. Zwerger, Many-body physics with ultracold gases, Rev. Mod. Phys. **80**, 885 (2008).

[5] M. J. Bijlsma, B. A. Heringa, and H. T. C. Stoof, Phonon exchange in dilute Fermi-Bose mixtures: Tailoring the Fermi-Fermi interaction, Phys. Rev. A **61**, 053601 (2000).

[6] H. Heiselberg, C. J. Pethick, H. Smith, and L. Viverit, Influence of Induced Interactions on the Superfluid Transition in Dilute Fermi Gases, Phys. Rev. Lett. **85**, 2418 (2000).

[7] D. V. Efremov and L. Viverit, *p*-wave Cooper pairing of fermions in mixtures of dilute Fermi and Bose gases, Phys. Rev. B **65**, 134519 (2002).

[8] L. Viverit, Boson-induced *s*-wave pairing in dilute boson-fermion mixtures, Phys. Rev. A **66**, 023605 (2002).

[9] F. Matera, Fermion pairing in Bose-Fermi mixtures, Phys. Rev. A **68**, 043624 (2003).

[10] T. Enss and W. Zwerger, Superfluidity near phase separation in Bose-Fermi mixtures, Eur. Phys. J. B **68**, 383 (2009).

[11] I. Titvinidze, M. Snoek, and W. Hofstetter, Generalized dynamical mean-field theory for Bose-Fermi mixtures in optical lattices, Phys. Rev. B **79**, 144506 (2009).

[12] P. Anders, P. Werner, M. Troyer, M. Sigrist, and L. Pollet, From the Cooper Problem to Canted Supersolids in Bose-Fermi Mixtures, Phys. Rev. Lett. **109**, 206401 (2012).

[13] M. Bukov and L. Pollet, Mean-field phase diagram of the Bose-Fermi Hubbard model, Phys. Rev. B **89**, 094502 (2014).

[14] T. Bilitewski and L. Pollet, Exotic superconductivity through bosons in a dynamical cluster approximation, Phys. Rev. B **92**, 184505 (2015).

[15] R. S. Christensen, J. Levinsen, and G. M. Bruun, Quasiparticle Properties of a Mobile Impurity in a Bose-Einstein Condensate, Phys. Rev. Lett. **115**, 160401 (2015).

[16] J. Levinsen, M. M. Parish, and G. M. Bruun, Impurity in a Bose-Einstein Condensate and the Efimov Effect, Phys. Rev. Lett. **115**, 125302 (2015).

[17] Z. Wu and G. M. Bruun, Topological Superfluid in a Fermi-Bose Mixture with a High Critical Temperature, Phys. Rev. Lett. **117**, 245302 (2016).

[18] J. M. Midtgaard, Z. Wu, and G. M. Bruun, Topological superfluidity of lattice fermions inside a Bose-Einstein condensate, Phys. Rev. A **94**, 063631 (2016).

[19] J. J. Kinnunen, Z. Wu, and G. M. Bruun, Induced *p*-Wave Pairing in Bose-Fermi Mixtures, Phys. Rev. Lett. **121**, 253402 (2018).

[20] S. M. Yoshida, S. Endo, J. Levinsen, and M. M. Parish, Universality of an Impurity in a Bose-Einstein Condensate, Phys. Rev. X **8**, 011024 (2018).

[21] M. Pierce, X. Leyronas, and F. Chevy, Few Versus Many-Body Physics of an Impurity Immersed in a Superfluid of Spin 1/2 Attractive Fermions, Phys. Rev. Lett. **123**, 080403 (2019).

[22] M. A. Cazalilla, R. Citro, T. Giamarchi, E. Orignac, and M. Rigol, One dimensional bosons: From condensed matter systems to ultracold gases, Rev. Mod. Phys. **83**, 1405 (2011).

[23] K. K. Das, Bose-Fermi Mixtures in One Dimension, Phys. Rev. Lett. **90**, 170403 (2003).

[24] M. A. Cazalilla and A. F. Ho, Instabilities in Binary Mixtures of One-Dimensional Quantum Degenerate Gases, Phys. Rev. Lett. **91**, 150403 (2003).

[25] L. Mathey, D.-W. Wang, W. Hofstetter, M. D. Lukin, and Eugene Demler, Luttinger Liquid of Polarons in One-Dimensional Boson-Fermion Mixtures, Phys. Rev. Lett. **93**, 120404 (2004).

[26] A. Imambekov and E. Demler, Exactly solvable case of a one-dimensional Bose-Fermi mixture, Phys. Rev. A **73**, 021602(R) (2006).

[27] L. Pollet, M. Troyer, K. Van Houcke, and S. M. A. Rombouts, Phase Diagram of Bose-Fermi Mixtures in One-Dimensional Optical Lattices, Phys. Rev. Lett. **96**, 190402 (2006).

[28] L. Mathey and D.-W. Wang, Phase diagrams of one-dimensional Bose-Fermi mixtures of ultracold atoms, Phys. Rev. A **75**, 013612 (2007).

[29] P. Sengupta and L. P. Pryadko, Quantum degenerate Bose-Fermi mixtures on one-dimensional optical lattices, Phys. Rev. B **75**, 132507 (2007).

[30] M. Rizzi and A. Imambekov, Pairing of one-dimensional Bose-Fermi mixtures with unequal masses, Phys. Rev. A **77**, 023621 (2008).

[31] A. Mering and M. Fleischhauer, One-dimensional Bose-Fermi-Hubbard model in the heavy-fermion limit, Phys. Rev. A **77**, 023601 (2008).

[32] F. M. Marchetti, T. Jolicoeur, and M. M. Parish, Stability and Pairing in Quasi-One-Dimensional Bose-Fermi Mixtures, Phys. Rev. Lett. **103**, 105304 (2009).

[33] E. Orignac, M. Tsuchiizu, and Y. Suzumura, Competition of superfluidity and density waves in one-dimensional Bose-Fermi mixtures, Phys. Rev. A **81**, 053626 (2010).

[34] B. Fang, P. Vignolo, M. Gattobigio, C. Miniatura, and A. Minguzzi, Exact solution for the degenerate ground-state manifold of a strongly interacting one-dimensional Bose-Fermi mixture, Phys. Rev. A **84**, 023626 (2011).

[35] I. Danshita and L. Mathey, Counterflow superfluid of polaron pairs in Bose-Fermi mixtures in optical lattices, Phys. Rev. A **87**, 021603(R) (2013).

[36] A. S. Dehkharghani, F. F. Bellotti, and N. T. Zinner, Analytical and numerical studies of Bose-Fermi mixtures in a one-dimensional harmonic trap, J. Phys. B **50**, 144002 (2017).

[37] B. Reichert, A. Petković, and Z. Ristivojevic, Quasiparticle decay in a one-dimensional Bose-Fermi mixture, Phys. Rev. B **95**, 045426 (2017).

[38] K. K. Nielsen, Z. Wu, and G. M. Bruun, Higher first Chern numbers in one-dimensional Bose–Fermi mixtures, New J. Phys. **20**, 025005 (2018).

[39] P. Siegl, S. I. Mistakidis, and P. Schmelcher, Many-body expansion dynamics of a Bose-Fermi mixture confined in an optical lattice, Phys. Rev. A **97**, 053626 (2018).

[40] D. Huber, H.-W. Hammer, and A. G. Volosniev, In-medium bound states of two bosonic impurities in a one-dimensional Fermi gas, arXiv:1908.02483.

[41] M. Singh and G. Orso, Enhanced visibility of the Fulde-Ferrel-Larkin-Ovchinnikov state in one dimensional Bose-Fermi mixtures near the immiscibility point, arXiv:1911.03448.

[42] L. D. Landau and S. I. Pekar, Effective mass of a polaron, J. Exp. Theor. Phys **18**, 419 (1948).

[43] H. Fröhlich, Electrons in lattice fields, Adv. Phys. **3**, 325 (1954).

[44] R. P. Feynman, Slow electrons in a polar crystal, Phys. Rev. **97**, 660 (1955).

[45] G. D. Mahan, *Many Particle Physics* (Springer, Berlin, 2000).

[46] M. Bruderer, A. Klein, S. R. Clark, and D. Jaksch, Polaron physics in optical lattices, Phys. Rev. A **76**, 011605(R) (2007).

[47] M. Schecter, D. M. Gangardt, and A. Kamenev, Dynamics and Bloch oscillations of mobile impurities in one-dimensional quantum liquids, Ann. Phys. (NY) **327**, 639 (2012).

[48] M. Schecter, A. Kamenev, D. M. Gangardt, and A. Lamacraft, Critical Velocity of a Mobile Impurity in One-Dimensional Quantum Liquids, Phys. Rev. Lett. **108**, 207001 (2012).

[49] W. Casteels, J. Tempere, and J. T. Devreese, Polaronic properties of an impurity in a Bose-Einstein condensate in reduced dimensions, Phys. Rev. A **86**, 043614 (2012).

[50] J. Bonart and L. F. Cugliandolo, From nonequilibrium quantum Brownian motion to impurity dynamics in one-dimensional quantum liquids, Phys. Rev. A **86**, 023636 (2012).

[51] J. Bonart and L. F. Cugliandolo, Effective potential and polaronic mass shift in a trapped dynamical impurity–Luttinger liquid system, Europhys. Lett. **101**, 16003 (2013).

[52] F. Massel, A. Kantian, A. J. Daley, T. Giamarchi, and P. Törmä, Dynamics of an impurity in a one-dimensional lattice, New J. Phys. **15**, 045018 (2013).

[53] S. Peotta, D. Rossini, M. Polini, F. Minardi, and R. Fazio, Quantum Breathing of an Impurity in a One-Dimensional Bath of Interacting Bosons, Phys. Rev. Lett. **110**, 015302 (2013).

[54] S. Dutta and E. J. Mueller, Variational study of polarons and bipolarons in a one-dimensional Bose lattice gas in both the superfluid and the Mott-insulator regimes, Phys. Rev. A **88**, 053601 (2013).

[55] A. Kantian, U. Schollwöck, and T. Giamarchi, Competing Regimes of Motion of 1D Mobile Impurities, Phys. Rev. Lett. **113**, 070601 (2014).

[56] T. Yin, D. Cocks, and W. Hofstetter, Polaronic effects in one- and two-band quantum systems, Phys. Rev. A **92**, 063635 (2015).

[57] A. S. Dehkharghani, A. G. Volosniev, and N. T. Zinner, Quantum impurity in a one-dimensional trapped Bose gas, Phys. Rev. A **92**, 031601(R) (2015).

[58] F. Grusdt and E. Demler, New theoretical approaches to Bose polarons, in *Quantum Matter at Ultralow Temperatures* (IOS Press, Amsterdam, The Netherlands, 2015).

[59] M. Schecter, D. M. Gangardt, and A. Kamenev, Quantum impurities: From mobile Josephson junctions to depletons, New J. Phys. **18**, 065002 (2016).

[60] A. Petković and Z. Ristivojevic, Dynamics of a Mobile Impurity in a One-Dimensional Bose Liquid, Phys. Rev. Lett. **117**, 105301 (2016).

[61] V. Pastukhov, Impurity states in the one-dimensional Bose gas, Phys. Rev. A **96**, 043625 (2017).

[62] A. G. Volosniev and H.-W. Hammer, Analytical approach to the Bose-polaron problem in one dimension, Phys. Rev. A **96**, 031601(R) (2017).

[63] L. Parisi and S. Giorgini, Quantum Monte Carlo study of the Bose-polaron problem in a one-dimensional gas with contact interactions, Phys. Rev. A **95**, 023619 (2017).

[64] F. Grusdt, G. E. Astrakharchik, and E. Demler, Bose polarons in ultracold atoms in one dimension: Beyond the Fröhlich paradigm, New J. Phys. **19**, 103035 (2017).

[65] S. I. Mistakidis, A. G. Volosniev, N. T. Zinner, and P. Schmelcher, Effective approach to impurity dynamics in one-dimensional trapped Bose gases, Phys. Rev. A **100**, 013619 (2019).

[66] J. Tempere, W. Casteels, M. K. Oberthaler, S. Knoop, E. Timmermans, and J. T. Devreese, Feynman path-integral treatment of the BEC-impurity polaron, Phys. Rev. B **80**, 184504 (2009).

[67] A. Privitera and W. Hofstetter, Polaronic slowing of fermionic impurities in lattice Bose-Fermi mixtures, Phys. Rev. A **82**, 063614 (2010).

[68] L. A. Peña Ardila and S. Giorgini, Impurity in a Bose-Einstein condensate: Study of the attractive and repulsive branch using quantum Monte Carlo methods, Phys. Rev. A **92**, 033612 (2015).

[69] Y. E. Shchadilova, R. Schmidt, F. Grusdt, and E. Demler, Quantum Dynamics of Ultracold Bose Polarons, Phys. Rev. Lett. **117**, 113002 (2016).

[70] F. Grusdt, R. Schmidt, Y. E. Shchadilova, and E. Demler, Strong-coupling Bose polarons in a Bose-Einstein condensate, Phys. Rev. A **96**, 013607 (2017).

[71] F. Grusdt, K. Seetharam, Y. Shchadilova, and E. Demler, Strong-coupling Bose polarons out of equilibrium: Dynamical renormalization-group approach, Phys. Rev. A **97**, 033612 (2018).

[72] L. A. Peña Ardila, G. E. Astrakharchik, and S. Giorgini, Strong coupling Bose polarons in a two-dimensional gas, arXiv:1907.01533.

[73] S. Palzer, C. Zipkes, C. Sias, and M. Köhl, Quantum Transport through a Tonks-Girardeau Gas, Phys. Rev. Lett. **103**, 150601 (2009).

[74] J. Catani, G. Lamporesi, D. Naik, M. Gring, M. Inguscio, F. Minardi, A. Kantian, and T. Giamarchi, Quantum dynamics of impurities in a one-dimensional Bose gas, Phys. Rev. A **85**, 023623 (2012).

[75] T. Fukuhara, A. Kantian, M. Endres, M. Cheneau, P. Schauß, S. Hild, D. Bellem, U. Schollwöck, T. Giamarchi, C. Gross, I. Bloch, and S. Kuhr, Quantum dynamics of a mobile spin impurity, Nat. Phys. **9**, 235 (2013).

[76] R. Scelle, T. Rentrop, A. Trautmann, T. Schuster, and M. K. Oberthaler, Motional Coherence of Fermions Immersed in a Bose Gas, Phys. Rev. Lett. **111**, 070401 (2013).

[77] M.-G. Hu, M. J. Van de Graaff, D. Kedar, J. P. Corson, E. A. Cornell, and D. S. Jin, Bose Polarons in the Strongly Interacting Regime, Phys. Rev. Lett. **117**, 055301 (2016).

[78] N. B. Jørgensen, L. Wacker, K. T. Skalmstang, M. M. Parish, J. Levinsen, R. S. Christensen, G. M. Bruun, and J. J. Arlt, Observation of Attractive and Repulsive Polarons in a Bose-Einstein Condensate, Phys. Rev. Lett. **117**, 055302 (2016).

[79] T. Rentrop, A. Trautmann, F. A. Olivares, F. Jendrzejewski, A. Komnik, and M. K. Oberthaler, Observation of the Phononic Lamb Shift with a Synthetic Vacuum, Phys. Rev. X **6**, 041041 (2016).

[80] Z. Z. Yan, Y. Ni, C. Robens, and M. W. Zwierlein, Bose polarons near quantum criticality, arXiv:1904.02685.

[81] J. Bardeen, G. Baym, and D. Pines, Effective interaction of He^3 atoms in dilute solutions of He^3 in He^4 at low temperatures, Phys. Rev. **156**, 207 (1967).

[82] A. S. Dehkharghani, A. G. Volosniev, and N. T. Zinner, Coalescence of Two Impurities in a Trapped One-Dimensional Bose Gas, Phys. Rev. Lett. **121**, 080405 (2018).

[83] S. Sarkar, S. McEndoo, D. Schneble, and A. J. Daley, Interspecies entanglement with impurity atoms in a bosonic lattice gas, arXiv:1805.01592.

[84] T. L. Schmidt, G. Dolcetto, C. J. Pedder, K. Le Hur, and P. P. Orth, Mechanical Resonances of Mobile Impurities in a One-Dimensional Quantum Fluid, Phys. Rev. Lett. **123**, 075302 (2019).

[85] S. I. Mistakidis, L. Hilbig, and P. Schmelcher, Correlated quantum dynamics of two quenched fermionic impurities immersed in a Bose-Einstein condensate, Phys. Rev. A **100**, 023620 (2019).

[86] S. I. Mistakidis, A. G. Volosniev, and P. Schmelcher, Induced correlations between impurities in a one-dimensional quenched Bose gas, arXiv:1911.05353.

[87] P. Naidon, Two impurities in a Bose-Einstein condensate: From Yukawa to Efimov attracted polarons, J. Phys. Soc. Jpn. **87**, 043002 (2018).

[88] A. Camacho-Guardian and G. M. Bruun, Landau Effective Interaction between Quasiparticles in a Bose-Einstein Condensate, Phys. Rev. X **8**, 031042 (2018).

[89] A. Camacho-Guardian, L. A. Peña Ardila, T. Pohl, and G. M. Bruun, Bipolarons in a Bose-Einstein Condensate, Phys. Rev. Lett. **121**, 013401 (2018).

[90] A. Recati, J. N. Fuchs, C. S. Peça, and W. Zwerger, Casimir forces between defects in one-dimensional quantum liquids, Phys. Rev. A **72**, 023616 (2005).

[91] P. Wächter, V. Meden, and K. Schönhammer, Indirect forces between impurities in one-dimensional quantum liquids, Phys. Rev. B **76**, 045123 (2007).

[92] M. Schecter and A. Kamenev, Phonon-Mediated Casimir Interaction between Mobile Impurities in One-Dimensional Quantum Liquids, Phys. Rev. Lett. **112**, 155301 (2014).

[93] A. I. Pavlov, J. van den Brink, and D. V. Efremov, Phonon-mediated Casimir interaction between finite-mass impurities, Phys. Rev. B **98**, 161410(R) (2018).

[94] B. Reichert, Z. Ristivojevic, and A. Petković, The Casimir-like effect in a one-dimensional Bose gas, New J. Phys. **21**, 053024 (2019).

[95] B. Reichert, A. Petković, and Z. Ristivojevic, Field-theoretical approach to the Casimir-like interaction in a one-dimensional Bose gas, Phys. Rev. B **99**, 205414 (2019).

[96] A. S. Alexandrov and N. F. Mott, Bipolarons, Rep. Prog. Phys. **57**, 1197 (1994).

[97] J. R. Waldram, *Superconductivity of Metals and Cuprates* (CRC Press, Boca Raton, FL, 1996).

[98] J. T. Devreese and A. S. Alexandrov, Fröhlich polaron and bipolaron: Recent developments, Rep. Prog. Phys. **72**, 066501 (2009).

[99] U. Schollwöck, The density-matrix renormalization group in the age of matrix product states, Ann. Phys. (NY) **326**, 96 (2011).

[100] M. Dolfi, B. Bauer, S. Keller, A. Kosenkov, T. Ewart, A. Kantian, T. Giamarchi, and M. Troyer, Matrix product state applications for the alps project, Comput. Phys. Commun. **185**, 3430 (2014).

[101] E. Jeckelmann and S. R. White, Density-matrix renormalization-group study of the polaron problem in the Holstein model, Phys. Rev. B **57**, 6376 (1998).

[102] B. Reichert, A. Petkovic, and Z. Ristivojevic, Fluctuation-induced potential for an impurity in a semi-infinite one-dimensional Bose gas, arXiv:1907.02169.

[103] A. M. Rey, G. Pupillo, C. W. Clark, and C. J. Williams, Ultracold atoms confined in an optical lattice plus parabolic potential: A closed-form approach, Phys. Rev. A **72**, 033616 (2005).

[104] M. Valiente and D. Petrosyan, Two-particle states in the Hubbard model, J. Phys. B **41**, 161002 (2008).

[105] A. E. Feiguin, F. Heidrich-Meisner, G. Orso, and W. Zwerger, BCS-BEC crossover and unconventional superfluid order in one dimension, in *The BCS-BEC Crossover and the Unitary Fermi Gas* (Springer, Berlin, 2012), pp. 503–532.

[106] M. Flicker and E. H. Lieb, Delta-function Fermi gas with two-spin deviates, Phys. Rev. **161**, 179 (1967).

[107] E. Chalbaud, J.-P. Gallinar, and G. Mata, The quantum harmonic oscillator on a lattice, J. Phys. A **19**, L385 (1986).